Proceedings of the
Linnean Society of New South Wales

Vertebrate fauna of the Lower Devonian Rookery Limestone Member in central New South Wales

Carole J. Burrow[1], Yong Yi Zhen[2] and Patrick M. Smith[3,4]

[1]Biodiversity and Geosciences, Queensland Museum, 122 Gerler Rd, Hendra Qld 4011 AUSTRALIA (carole.burrow@gmail.com); [2]Geological Survey of New South Wales, 947–953 Londonderry Road, Londonderry NSW 2753 AUSTRALIA; [3]Palaeontology Department, Australian Museum Research Institute, Sydney NSW 2010 AUSTRALIA; [4]School of Natural Sciences, Macquarie University, Sydney NSW 2109 AUSTRALIA.

Natural History in all its Branches

Burrow, C.J., Zhen, Y.Y. and Smith, P.M. (2025) Vertebrate fauna of the Lower Devonian Rookery Limestone Member in central New South Wales. *Proceedings of the Linnean Society of New South Wales* **147**, 77-90.

Published on 7 December 2025 at https://openjournals.library.sydney.edu.au/index.php/LIN/index

Manuscript accepted for publication 24 October 2025

Keywords: *Nostovicina guangxiensis*, romundinid placoderm, *Connemarraspis*?, late Lochkovian, biostratigraphy, Meryula Formation, Lachlan Orogen

PO Box 291, Manly NSW 1655
https://linneansocietynsw.org.au
secretary@linneansocietynsw.org.au
0490 542 524

ISSN 1839-7263

ABSTRACT

The Rookery Limestone Member is exposed in a small area on ‘The Rookery’, southeast of Cobar in central NSW. An Early Devonian, either Lochkovian or Pragian, age for the stratum was previously determined based on the brachiopod, trilobite and conodont faunas preserved. Microvertebrate remains include scales of acanthodians *Nostovicina guangxiensis* and *Trundlelepis cervicostulata*; scales and dermal bone fragments possibly of the placoderm *Connemarraspis*; and scales, dermal bone fragments, and possible gnathal plates of a romundinid placoderm. Alternatively, the gnathal plates could be from the stem osteichthyan *Lophosteus incrementus*. This fauna indicates a late Lochkovian age based on the stratigraphic distribution of these taxa elsewhere in NSW, and accords with dating suggested by the conodont taxa from the same samples.

INTRODUCTION

Microvertebrate remains, including scales and dermal bone fragments of acanthodians and placoderms, have been recorded from several carbonate units of late Silurian to Early Devonian age in the Cobar Basin of central New South Wales (e.g., Basden *et al*. 2000; Burrow 1996, 1997, 2002, 2003a, 2006; Burrow *et al*. 2010; Zhen *et al*. 2023). They were recovered in association with conodonts and other microfossils in residues of limestone samples processed primarily for conodonts. This report gives a summary of the conodont taxa and a description of the microvertebrate remains recovered from the Early Devonian Rookery Limestone Member within the Meryula Formation exposed on ‘The Rookery’, located about 35 km SE of Cobar in central New South Wales. Microvertebrate remains are useful not only to solve the palaeobiological puzzles related to origin and evolution of these organisms but also can assist in dating and correlating the rocks bearing these fossils.

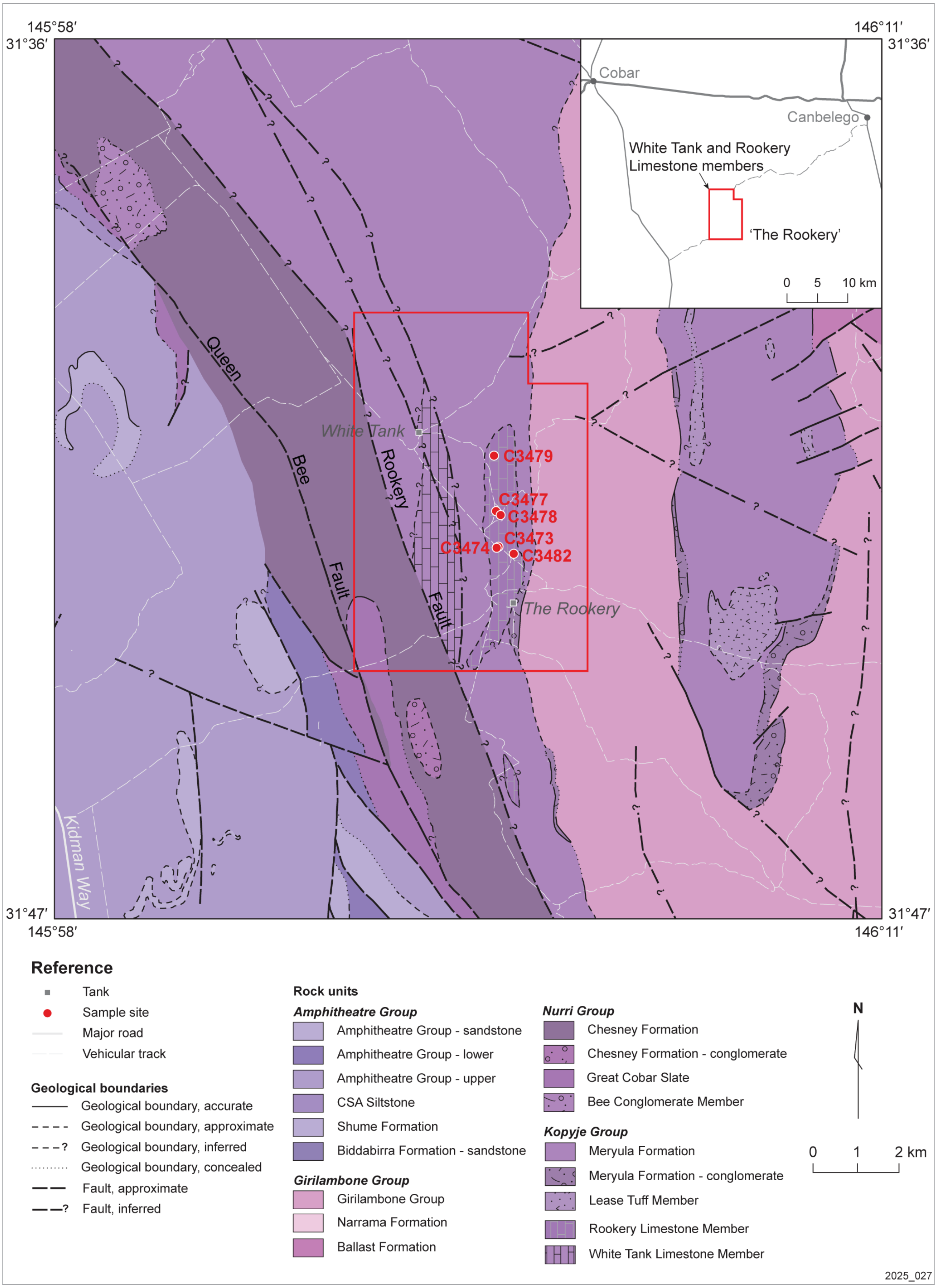

Figure 1. Simplified geology map in the vicinity of 'The Rookery' showing distribution of outcrops mapped as the White Tank and Rookery Limestone members of the Meryula Formation (after Colquhoun *et al.* 2024) and locations of the study samples from the Rookery Limestone Member.

GEOLOGICAL SETTING

The study area (Figure 1) is located immediately east of the Rookery Fault that separates the Cobar Trough to the west and the Kopyje Shelf to the east (Glen 1995; David 2005). Flanking the Cobar Trough, which is characterized by a turbiditic sequence (Amphitheatre Group), the Kopyje Shelf was the site of shallow-water deposition during the late Silurian to Early Devonian, which is represented by the Kopyje Group in the study area (Felton 1981; Glen 1994; Downes *et al*. 2016; Jones *et al*. 2020; Zhen *et al*. 2023). The Rookery Limestone Member and White Tank Limestone Member of the Meryula Formation are the only carbonate units within the Kopyje Group in the study area. These units comprise fossiliferous massive to well-bedded limestones with locally developed tabulate coral-stromatoporoid biostromes and bioherms, that crop out in patches on both side of the track from the homestead to White Tank. The cluster of outcrops exposed primarily to the west side of the track is mapped as the White Tank Limestone Member and those exposed to the east side of the track and homestead as the Rookery Limestone Member (Figure 1). They were deposited as a carbonate platform with patch reefs fringing a local topographic high (or highs) on the Kopyje Shelf during two separate episodes in the early and late Lochkovian.

ROOKERY LIMESTONE MEMBER AND ITS BIOSTRATIGRAPHY

Invertebrate fossils from limestones cropping out on 'The Rookery', which Andrews (1913, p. 37, 38) referred to as the Rookery Limestones, were examined by Etheridge and Dun (in Andrews 1913), who suggested a late Silurian age. These limestones were further differentiated by Pogson and Felton (1978, p. 7, Figure 2) as the Rookery Limestone Member and the White Tank Limestone Member, positioned respectively in the lower and upper parts of the Meryula Formation, the latter of predominantly poorly outcropping ferruginous siltstones with the basal conglomerates bearing pebbles derived from the underlying Ordovician rocks (Felton 1981, p. 70). Felton (1981) later formally defined these units as contemporaneous deposits, interpreting the White Tank Limestone Member as a reef facies developed to the west, and the Rookery Limestone Member as a back-reef facies developed to the east (Figure 1).

Based on the conodont faunas recovered from these two limestone members, Pickett (1980) assigned an earliest Lochkovian age to the White Tank Limestone Member, supported by the recovery of *Caudicriodus woschmidti* (Ziegler, 1960), and a late Lochkovian age to the Rookery Limestone Member, evidenced by the occurrence of *Pedavis pesavis* (Bischoff and Sannemann, 1958). The Rookery Limestone Member was then correlated with the lower Garra Formation that yielded a similar conodont fauna (Druce 1970). However, Mathieson *et al*. (2016) suggested a younger Pragian (*sulcatus* Biozone) age for both limestone members, based on a reassessment of the specimens described by Pickett (1980), with no new material examined. More specifically, Mathieson *et al*. (2016) indicated that the specimen figured by Pickett (1980, fig. 4E) as *Pedavis pesavis* was instead a younger species, although this was done without providing a species assignment or further comparisons. In an attempt to resolve these conflicting age estimates, further collecting in 2024 by Zhen and Smith yielded a similar fauna (Figure 2) to that documented by Pickett (1980), as detailed below.

The small suite of microvertebrate remains from the Rookery Limestone Member, described below in the Systematic Palaeontology section, also indicate a late Lochkovian age when compared with the stratigraphic distribution of these taxa elsewhere in NSW.

MATERIALS AND METHODS

The microvertebrate remains documented in this report are from five samples with an average weight of 5 kg, including C3473 (Lat. -31.712136875°, Long. 146.077723064°), C3474 (Lat. -31.712370209°, Long. 146.077256397°), C3477 (Lat. -31.704670208°, Long. 146.077189731°), C3478 (Lat. -31.705503542°, Long. 146.078306398°) and C3479 (Lat. -31.693020208°, Long. 146.076806399°) from the Rookery Limestone Member (Fig. 1). Conodonts illustrated in Figure 2 are associated with the microvertebrate remains documented, except for the specimen representing the Pa element (Fig. 2m) of *Pedavis pesavis* which is from sample C3482 (Lat. -31.713653542°, Long. 146.081439730°). Representative forms of the microvertebrate fauna are illustrated in Figures 3–6. Algal/fungal hyphal borings were noted in all the microvertebrate specimens. Samples were processed at the Palaeontology Lab of the Geological Survey of New South Wales (GSNSW) located in the WB Clarke Geoscience Centre at Londonderry in western Sydney, using diluted (10%) Acetic Acid and were separated using Sodium Polytungstate solution to reduce the residue volume prior to picking. All the 49 studied microvertebrate remains and conodont specimens are deposited in the GSNSW Fossil Collection at Londonderry, including 45 figured specimens (Figures 2–6) and four unfigured specimens of microvertebrate remains that have been photographed by SEM and used in the study. They bear the prefix MMMC (MMMC006253 to MMMC06301). Institutional abbreviations: GSNSW, Geological Survey of New South Wales; MMMC, microfossil collection of the GSNSW.

DESCRIPTION OF NEW CONODONT MATERIAL

The new samples from the Rookery Limestone Member includes abundant *Amydrotaxis druceana* (Pickett, 1980) (Fig. 2a–e), *Zieglerodina remscheidensis* (Ziegler, 1960 (Fig. 2f–h), and *Panderodus unicostatus* (Branson and

Mehl, 1933) (Fig. 2i). *Oulodus* sp. cf. *Oul. walliseri* Ziegler, 1960 (Fig. 2i) is common and *Belodella resima* (Philip, 1965) (Fig. 2j) and *Belodella* sp. (Fig. 2k) are relatively rare. A few specimens of *Pedavis pesavis* (Fig. 2m) recovered from one of our new samples have a more or less straight extending posterior process, resembling the specimens of this species reported from the McMonnigal Limestone in Nevada (Klapper and Philip 1971, fig. 14I) and *Pedavis breviramus* Murphy and Matti, 1982 reported by Valenzuela-Ríos *et al*. (2017, fig. 4.9) from northern Spain. *Pedavis breviramus* may be a direct ancestor to *Pedavis pesavis*, and thus has a stratigraphic range that precedes it (see Valenzuela-Ríos *et al*. 2017, fig. 3). The holotype of *Pedavis pesavis* has a distally strongly curved posterior process (Bischoff and Sannemann 1958, pl. 12, fig. 1). However, the length and curvature of the posterior process of *Pedavis pesavis* varies significantly amongst specimens illustrated by Bischoff and Sannemann (1958, pl. 12, figs 2–4, 6, 7). The *Pedavis pesavis* specimen illustrated by Pickett (1980, fig. 4E) bears an inner-laterally weakly flexed posterior process and is identical with this zonal index species as illustrated by Valenzuela-Ríos *et al*. (2017, figs 3, 4.11) from northern Spain. Therefore, occurrence of *Pedavis pesavis* in the Rookery Limestone Member is age diagnostic supporting a late Lochkovian age.

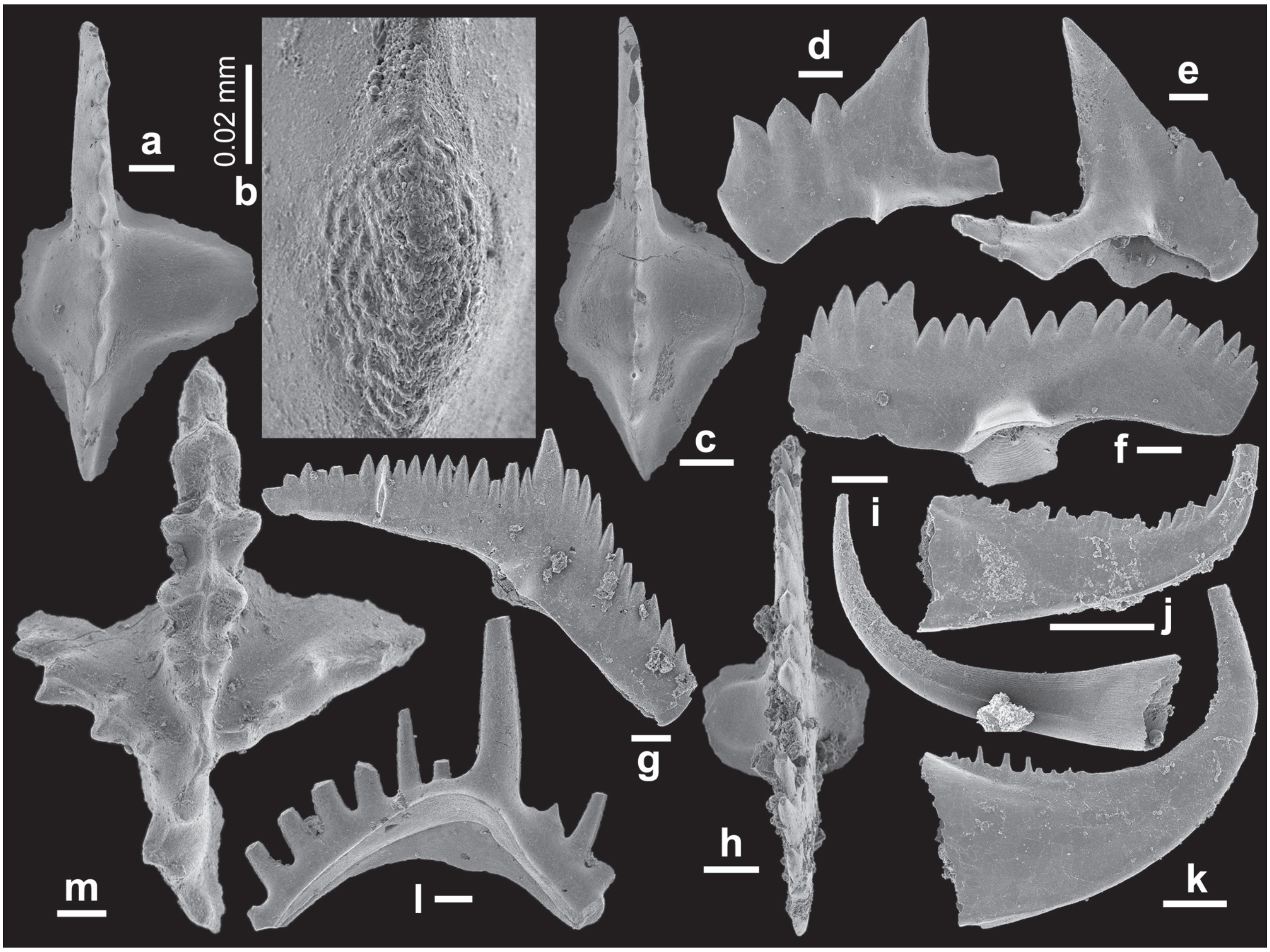

Figure 2. Conodonts associated with microvertebrate remains from the Rookery Limestone Member within the Meryula Formation exposed near Cobar. a–e, *Amydrotaxis druceana* (Pickett, 1980); a, b, Pa element, MMMC06253, from sample C3473, a, apical view (IY491-06 C3473), b, close-up showing microsculpture on the node (IY491-007); c, Pa element, MMMC06254, from sample C3473, apical view (IY491-013); d, Pb element, MMMC06255, from sample C3473, outer-lateral view (IY491-014); e, Pb element, MMMC06256, from sample C3473, inner-lateral view (IY491-018). f–h, *Zieglerodina remscheidensis* (Ziegler, 1960); f, Pa element, MMMC06257, from sample C3473, inner-lateral view (IY491-020); g, Pb element, MMMC06258, from sample C3473, inner-lateral view (IY491-022); h Pa element, MMMC06259, from sample C3473, apical view (IY491-021). i, *Panderodus unicostatus* (Branson and Mehl, 1933), qg element, MMMC06260, from sample C3473, inner-lateral view (IY494-023). j, *Belodella resima* (Philip, 1965); Sa element, MMMC06261, from sample C3474, lateral view (IY494-011). k, *Belodella* sp., Sc element, MMMC06262, from sample C3473, outer-lateral view (IY494-020). l, *Oulodus* sp. cf. *Oul. walliseri* Ziegler, 1960; Pa element, MMMC06263, from sample C3473, posterior view (IY494-019). m, *Pedavis pesavis* (Bischoff and Sannemann, 1958), Pa element, MMMC06264, from sample C3482, apical view (IY500-001). Scale bars = 200 µm, unless otherwise indicated.

SYSTEMATIC PALAEONTOLOGY

GNATHOSTOMATA Gegenbaur, 1874
'PLACODERMI' M'Coy, 1848
ACANTHOTHORACI Stensiö, 1944

Remarks

Recent phylogenetic analyses of early gnathostomes have mostly resolved the placoderms as a grade of stem gnathostomes, though these analyses have poor statistical support (e.g. Brazeau *et al*. 2020). Similarly, the Acanthothoraci (sensu Stensiö 1944) have more recently been considered a grade rather than a clade within the "Placodermi" (Vaškaninová *et al*. 2020), but again, without strong support. Brazeau *et al*. (2023), in an analysis revised from that of Vaškaninová *et al*. (2020), eliminated taxa for which mandibular characters were unknown, giving a result with an acanthothoracid clade (*Romundina*, *Kosoraspis* and *Radotina*) identified by two unambiguous synapomorphies: the presence of a ventral notch between the parachordals, and the absence of complete dermal encirclement of the pectoral fin base.

Genus *Romundina Ørvig*, 1975

Type species

Romundina stellina Ørvig, 1975

Remarks

The original description of this monospecific genus did not include a formal diagnosis. Although Denison (1978, p. 36) listed several notable features, subsequent work has shown that multiple, closely related taxa likely co-occur at the type locality. One of these taxa, *Romundina gagnieri* Olive, Kotoulas, Goujet *et al*., 2025 was very recently described, the holotype being MNHN.F.CPW9, a specimen first figured by Goujet and Young (2004, fig. 3A: 'acanthothoracid') and several authors subsequently. Olive *et al*. (2025) provided diagnoses for *Romundina* and the new species, but these only list features of the skull, with the "ornamentation with stellate semidentine odontodes" as a generic character. It still thus remains uncertain which post-cranial morphological characters correspond to which species, or genus. Consequently, our assignment of the Rookery Limestone Member specimens to this genus is tentative.

***Romundina*? sp.**
(Figs. 3, 4a–d)

Referred material

Scales MMMC06265, from sample C3474 (IY499-012, Fig. 3a), MMMC06266 from sample 3474 (IY493-024, Fig. 3b), MMMC06267 from sample 3474 (IY493-022, Fig. 3c), MMMC06268 from sample C3474 (IY493-023, Fig. 3d), MMMC06269, from sample C3473 (IY499-017, Fig. 3e), MMMC06270 from sample C3477 (IY498-008, Fig. 3f), MMMC06271 from sample C3474 (IY497-016, Fig. 3g), ?MMMC06279 from sample C3474 (IY497-015, Fig. 3o), ?MMMC06278 from sample C3477 (IY498-009, Fig. 3n), ?MMMC06299 from sample C3474 (IY499-015); plates and plate fragments MMMC06716 from sample C3473 (IY499-016), MMMC06272 from sample C3473 (IY499-018, Fig. 3h), MMMC06298 from sample C3476 (IY498-012), MMMC06273 from sample C 3479 (IY499-019, Fig. 3i), MMMC06274 from sample 3474 (IY493-025, Fig. 3j), MMMC06301 from sample C3475 (IY498-010), MMMC06276 from sample C3474 (IY499-013, Fig. 3l), MMMC06277 from sample C3474 (IY499-001, Fig. 3m), MMMC06275 from sample C3478 (IY497-014, Fig. 3k); probably apronic (postbranchial) lamina fragments MMMC06280 from sample C3479 (IY498-004, Fig. 4a), MMMC06282 from sample C3474 (IY499-007, Fig. 4c), MMMC06281 from sample C3479 (IY499-020, Fig. 4b); and spinal plate fragment MMMC06283 from sample C3479 (IY498-005, Fig. 4d).

Description

Scales show a wide range of sizes and shapes and ornament arrangement (Fig. 3a–g). They have a square, elongate rhombic, or sub-polygonal outline, and are from c. 0.4 mm to 2.0 mm wide/long. The crown ornament comprises stellate tubercles with nodose ridges radiating from the apex. The number of ridges is highly variable, with the largest tubercles (c. 0.5 mm wide; Fig. 3g) having >12, some of which bifurcate towards the base. Smallest tubercles, found towards the scale edge, are <0.1 mm wide (Fig. 3c–e), with perhaps two ridges. There are c. six tiny nodes per 0.1 mm on the ridges. Tubercles are mostly contiguous, but do not overlap or overgrow adjacent tubercles. They can be upright or inclined, presumably dependent on the position of the scale on the body. Pores open out on the surface of the scale between the tubercles. An ornament free outer edge extends around the whole or only part of the scale. Base of the scale is only slightly convex.

Most of the dermal plates and plate fragments found (Fig. 3h–m) bear the same type of ornament tubercles as the scales, but are distinguished from scales by their larger size (Fig. 3h–j), presence of open sensory canals (Fig. 3i), or having a cancellous layer between the ornament layer and the base (e.g. Fig. 3l). Some specimens (Fig. 3n, 3o) are only tentatively assigned to this taxon, as the tubercle ridges are not, or are only minimally, noded.

Dermal bone fragments (Fig. 4a–c) which bear only distinctive triangular tubercles are characteristic of the apronic postbranchial lamina on the anterolateral and anteroventral plates of the *Romundina* trunk armour. These tubercles are strongly inclined, with serrated margins on the two free edges; the tubercle bases are c. 0.4 mm long, increasing in height away from the unornamented anterior edge of the plates (Fig. 4a–c). The distinctive fragment MMMC06283 (Fig. 4d) is part of a spinal plate with ornamented sides separated by a smooth ridge. This is comparable with the only asymmetrical spine-like dermal plate known for *Romundina stellina* (see Ørvig 1975, pl. 5 figs. 8, 9), where the spinal plate is fused to the other plates forming the trunk armour.

Comparison

The type species *Romundina stellina* is from the middle Lochkovian on Prince of Wales Island, Canadian

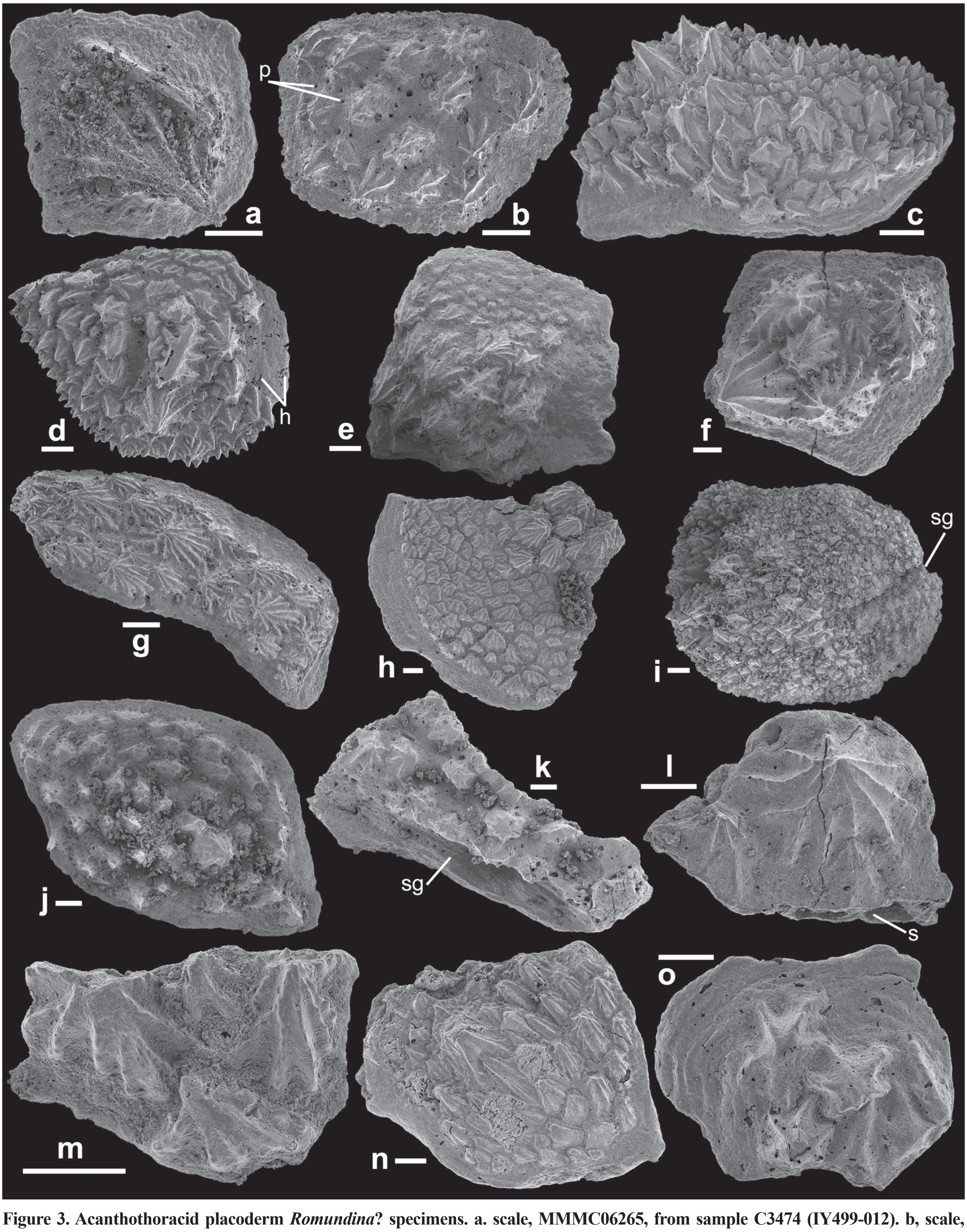

Figure 3. Acanthothoracid placoderm *Romundina*? specimens. a. scale, MMMC06265, from sample C3474 (IY499-012). b, scale, MMMC06266, from sample C3474 (IY493-024). c, scale, MMMC06267, from sample C3474 (IY493-022). d, scale, MMMC06268, from sample C3474 (IY493-023). e, scale, MMMC06269, from sample C3473 (IY499-017). f, scale, MMMC06270, from sample C3477 (IY498-008), with large tubercles. g, scale, MMMC06271, from sample C3474 (IY497-016). h, broken plate, MMMC06272, from sample C3473 (IY499-018). i, plate, MMMC06273, from sample C3479 (IY499-019) with sensory groove. j, plate, MMMC06274, from sample C3474 (IY493-025). k, plate fragment, MMMC06275, from sample C3478 (IY497-014). l, dermal bone fragment, MMMC06276, from sample C3474 (IY499-013). m, dermal bone fragment, MMMC06277, from sample C3474 (IY499-001). n, plate, MMMC06278, from sample C3477 (IY498-009), possibly *Romundina*?. o, scale, MMMC06279, from sample C3474 (IY497-015), possibly *Romundina*?. h, hyphal boring; p, pore; s, spongiosa layer; sg, sensory groove. Scale bars = 200 µm.

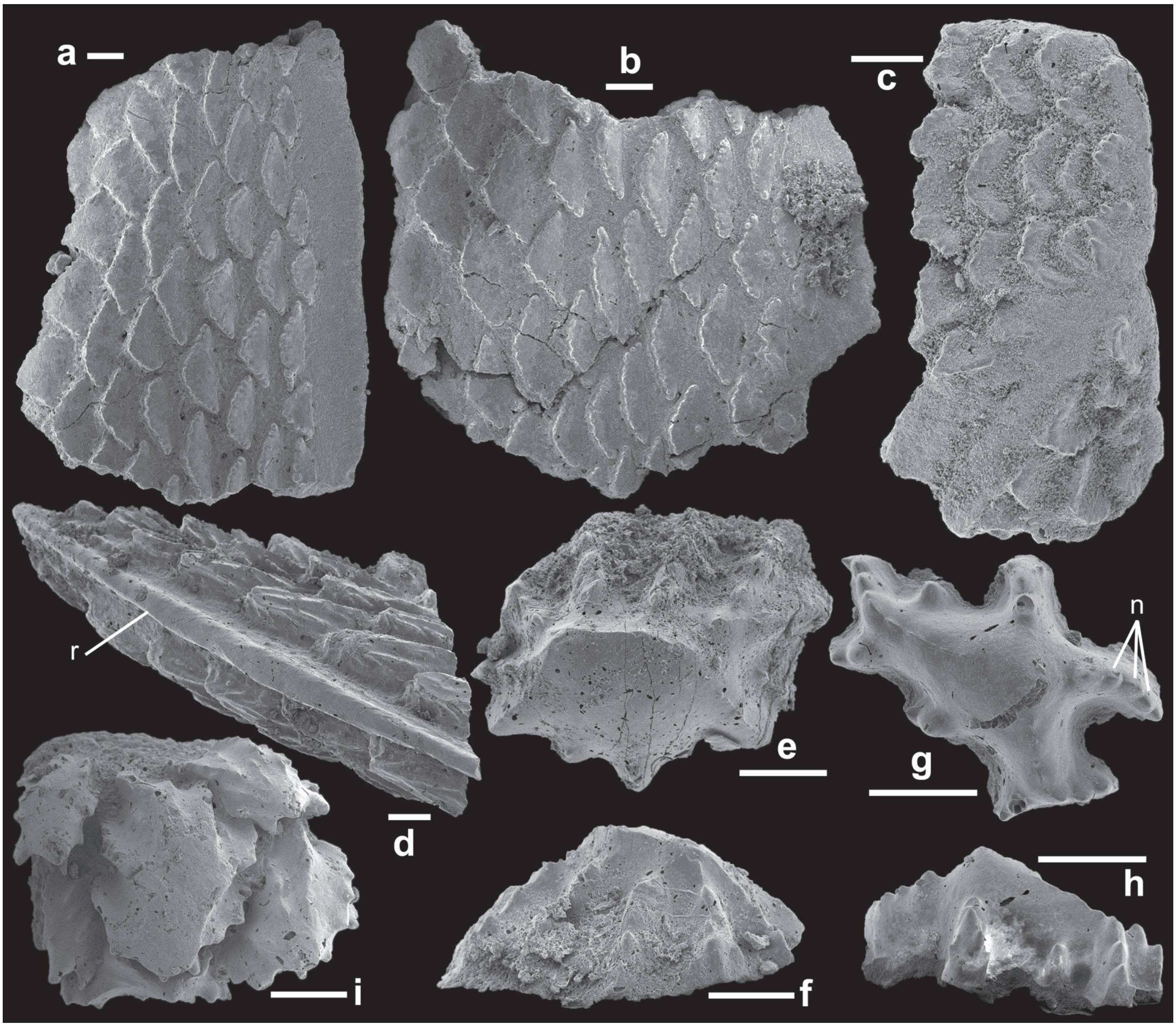

Figure 4. Acanthothoracid placoderm specimens. a–d, *Romundina*? sp. a–c, apronic (postbranchial) lamina fragments; a, MMMC06280, from sample C3479 (IY498-004); b, MMMC06281, from sample C3479 (IY499-020); c, MMMC06282, from sample C3474 (IY499-007); a and b appear to be dorsal and ventral parts of a larger plate fragment. d, Spinal plate fragment MMMC06283, from sample C3479 (IY498-005). e–i, *Connemarraspis*? scale/dermal bone fragments; e, f, single large tubercle, MMMC06284, from sample C3474, e, crown view (IY499-003), f, lateral view (IY499-022). g, h, single large tubercle, MMMC06285, from sample C3474, g, crown view (IY499-006), h, lateral view (IY499-023). i, dermal bone fragment, MMMC06286, from sample C3474 (IY499-010). n, node; r, ridge. Scale bars = 200 µm.

Arctic Archipelago. Other semi-articulated romundinid specimens are also known from Lochkovian deposits in the Northwest Territories, Canada (Johanson and Smith 2003, fig. 8) and Pechora Province, Norilsk region, and Novaya Sibir Island in Russia (Mark-Kurik 1988, fig. 49, pl. 17 fig. 18). The variation in ornament on dermal bones of *Romundina stellina* was well illustrated by Ørvig (1975, pls. 1–7), with his plate 6 figuring SEM images of the ornament tubercles on the dermal bones, and his plate 7 figuring SEM images of the ornament on the apronic (postbranchial) lamina, with the same type of triangular tubercles as on the Rookery Limestone Member specimens. Johanson and Smith (2003, fig. 8) illustrated the ornament on the anterior trunk shield of *Romundina* sp. from the Lochkovian Man-on-the-Hill locality in Northwest Territories, Canada, in a description of the postbranchial lamina ornament known from this and other placoderms. The tubercles in this area could be distinguished from those on the other taxa illustrated. Burrow and Turner (1999, fig. 3A, 3B) showed the morphology and histology of small plates or scales associated with the holotype. Rücklin and Donoghue (2015, fig. 1b–e) illustrated surface renderings of a plate (misidentified as a supragnathal dental plate) associated with the holotype of *R. stellina*, as well as of a scale (Rücklin and Donoghue 2015, fig. 2f, g). Burrow *et al*. (2016) suggested that plate possibly came from the mosaic of small ornamented plates in the *Romundina* ventral armour (see Goujet and Young 2004, fig. 4). Plate MMMC06273 (Fig. 3i) resembles the plate figured by Rücklin and Donoghue (2015).

Elsewhere in the world, romundinid scales and dermal plates have also been illustrated from the Lochkovian Windmill Limestone in Nevada (Turner and Murphy 1988, fig. 2.8–2.12: captioned as ‘placoderm scales’; Parkes 1995, fig. 24: captioned as ‘*Romundina stellina*’ and other indeterminate placoderms). Wang (1993, tab. 3) reported scales of *R. stellina* from the Lochkovian of the Luesma and Nogueras formations in Celtiberia, Spain, but did not describe or figure specimens. However, some dermal bone fragments of the same age that he assigned to *Ohioaspis tumulosa* Wells, 1944 (Wang 1993, pl. 3 figs. 4, 10) could rather be from a romundinid as they bear simple noded, stellate tubercles.

The scale and dermal bone material (including the postbranchial lamina fragments) from the Rookery Limestone Member falls within the range of morphologies exhibited by the type and other material assigned to *Romundina*. In New South Wales, scales and plates comparable to those

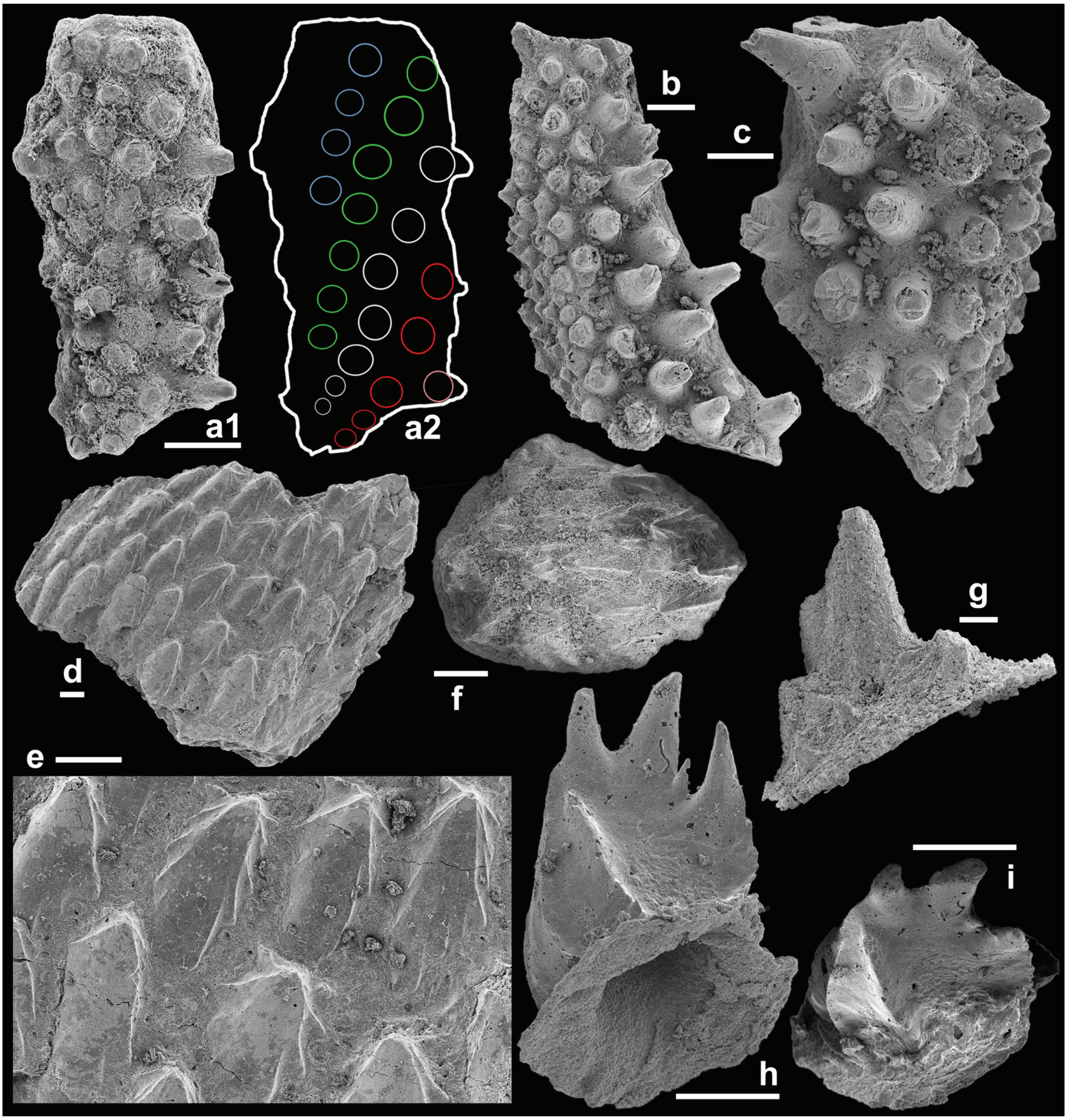

Figure 5. Gnathostome indet., acanthothoracid placoderm or lophosteid specimens. a–c, denticulated/toothed gnathal bones. a1, MMMC06287, from sample C3474 (IY499-002); a2, sketch showing distribution of denticle/tooth rows; b, MMMC06288, from sample C3479 (IY498-007); c, MMMC06289, from sample C3479 (IY498-006). d, e, dermal bone fragment, whole specimen and close-up view of tubercles, d, MMMC06290, from sample C3478 (IY497-012); e, close-up of the same specimen (IY497-013). f, gen. et sp. indet. A, scale, MMMC06291, from sample C3474 (IY493-026). g, gen. et sp. indet. B, scale, MMMC06292, from sample C3479 (IY499-021). h, i, gen. et sp. indet. C, scale, MMMC06293, from sample C3474, h, lateral view (IY499-011), I, oblique crown view (IY499-026). Scale bars = 200 µm.

of the type specimens have also been recovered from: the lower Lochkovian Cookeys Plains Formation (Burrow 2003a, fig. 5A–F); the lowermost beds (Lochkovian, *pesavis* CZ) of the Garra Limestone (Basden *et al*. 2000, fig. 4.1, 4.10, 4.11: captioned as 'Placoderm 9', and fig. 7.1, 7.3, 7.4: captioned as 'Murrindalaspid?'); the lower to middle Lochkovian Windellama Limestone (Basden *et al*. 2000, fig. 3: captioned as various placoderms; their fig. 3.12 is a post-branchial lamina fragment with identical ornament to that figured here); and the upper Lochkovian Connemarra Formation (Burrow *et al*. 2010, fig. 5N). No records are known for occurrences of romundinids in deposits younger than Lochkovian with one exception – Burrow *et al*. (1998) noted that some dermal bone fragments from the lower Pragian of the Point Hibbs Limestone, western Tasmania, resembled that of *R. stellina*.

Genus *Connemarraspis* Burrow, 2006

Type species
Connemarraspis youngi Burrow, 2006

Diagnosis
Dermal bone and scale ornament comprises small (0.2-0.4 cm wide) stellate tubercles and large circular or elongate flat-topped tubercles with lateral ridges; scales bear tubercles similar to those on the dermal plates, and lack isopedin in the base (for tubercle morphology, after Burrow 2006).

***Connemarraspis*? sp.**
Figure 4e–i

Referred material
Scales or isolated tubercles MMMC06284 from sample C 3474 (IY499-003, IY499-022, Fig. 4e, 4f), MMMC06285 from sample C 3474 (IY499-006, IY499-023, Fig. 4g, 4h), MMMC06286 from sample C 3474 (IY499-010, Fig. 4i).

Description
These three elements have distinctive robust tubercles up to 0.8 mm long/wide, interpreted here as comparable to unabraded tubercles on scales and dermal plates of *C. youngi* (Burrow 2006, figs. 6E, 8A; Basden *et al*. 2000, figs. 4.5–4.8, 7.2). The two scales with single tubercles (Fig. 4e–h) have noded ridges radiating out from the apex of the single tubercle; nodes are up to 0.1 mm diameter at the base, notably larger than those on *Romundina* tubercles.

Comparison
The type material of *Connemarraspis youngi* is from the Lochkovian Connemarra Formation near Trundle, central New South Wales; other occurrences in New South Wales are in the mid to late Lochkovian section of the Garra Formation and the early Lochkovian Camelford Limestone (Basden *et al*. 2000). The species also possibly was present in the ?Pragian Point Hibbs Formation, western Tasmania (Burrow *et al*. 1998, fig. 4D-J). The taxon has not been recorded from outside Australia. Tubercles similar in morphology and size to those typical of *Connemarraspis* are also found on some dermal plates of romundinids, in particular the premedian plate of acanthothoracid CPW.9A (Goujet and Young 2004, fig. 3A) and spinal plate of *Romundina* sp. (Johanson and Smith 2003, fig. 8F), but no romundinid scales are known to have this type of tubercle.

GNATHOSTOMATA, indet. gen. et sp.
Figure 5a–i

Referred material
Gnathal plates MMMC06287 from sample C 3474 (IY499-002, Fig. 5a), MMMC06288 from sample C 3474 (IY498-007, Fig. 5b), MMMC06289 from sample C 3479 (IY498-006, Fig. 5c), plate fragment MMMC06290 from sample C 3478 (IY497-012, IY497-013, Fig. 5d, 5e); scales MMMC06291 from sample C 3474 (IY493-026, Fig. 5f), MMMC06292 from sample C 3479 (IY499-021, Fig. 5g), MMMC06293 from sample C3474 (IY499-011, IY499-026, Fig. 5h, 5i).

Description
The three gnathal plates (Fig. 5a–c) have an upturned U-shaped cross section; none appear to be whole, with fracture surfaces visible on both ends of plates MMMC06287 and MMMC06289, and one end of MMMC06288. The plates bear smooth upright denticles/teeth, arranged in oblique rows across the 'crest' of the plate (Fig. 5a), increasing in size towards the slightly concave, presumed lingual, edges of the plates. Labially, the denticles are smaller and appear more randomly distributed. The apices have broken off or are worn away on most of the larger denticles/teeth, showing that they lack a large inner pulp cavity. Smaller canals are cut across on some of the tubercle fracture surfaces; as on the scales, algal or fungal hyphal borings also commonly penetrate the fossils.

Plate fragment MMMC06290 (Fig. 5d, 5e) has a transversely concave base. The strongly inclined ornament tubercles are 0.5–0.7 mm long and c. 0.3 mms wide, more or less arranged in longitudinal rows. The tubercles have a smooth central area and c. 10 thin sharp lateral ridges radiating back from the apex. Small nodes are rarely visible on ridges (Fig. 5e). Subpolygonal scale indet. gen. et sp. A, MMMC06291 (Fig. 5f) is poorly preserved, lacks an ornament-free margin, and bears strongly inclined tubercles c. 0.3 mm long, with seven or fewer ridges radiating from the apex.

Scale indet. gen. et sp. B, MMMC06292 (Fig. 5g) is very poorly preserved. It has a flat base, and a large central tubercle c. 1.0 mm high, with a few smaller tubercles around it. Scale indet. gen. et sp. C, MMMC06293 (Fig. 5h, 5i) is a very distinctive monodontode scale with a large central pulp cavity opening out through the base (Fig. 5h). The crown resembles a cock's comb, with high sharp projections extending out from one of the vertical ridges.

Comparison
When Burrow (1995) assigned tooth plates like those illustrated in Figure 4a-c to a new species *Lophosteus incrementus*, similar tooth plates had only previously been assigned to the stem osteichthyan *Lophosteus* Gross, 1969.

In recent years however, multiple such plates have been described from the upper jaw dentition of some articulated placoderm specimens, including the acanthothoracid *Kosoraspis peckai* Gross, 1959 (Vaškaninová *et al*. 2020, fig. 3). However, the only gnathal plates reliably assigned to a romundinid are the distinctive anterior supragnathal plates on the articulated *Romundina gagnieri* holotype CPW.9A from the *R. stellina* type locality (Goujet and Young 2004, fig. 3A; Smith and Johanson 2017, figs. 1, 2A, 2B; Olive et al. 2025, fig. 2). These differ from the Rookery Limestone Member and *K. peckai* plates in having a flat to slightly concave aboral surface which aligned with the surface of the ethmoid region of the braincase. It seems likely that romundinids also had plates like those of *K. peckai* which straddled the upper jaw cartilages, but as yet they have not been identified, or at least not identified in association with the *Romundina* type specimens. However, Burrow (2003b, fig. 1A: 'acanthothoracid placoderm') illustrated an isolated gnathal plate with the same general layout as the Rookery Limestone Member and *K. peckai* plates which, like the *Romundina* type material, is from the Lochkovian of Prince of Wales Island.

The Rookery Limestone Member gnathal plates (and also those assigned to *L. incrementus* by Burrow 1995) differ from those of the *Lophosteus* type species *L. superbus* (e.g. Gross 1969, fig. 9) in lacking a zone of weakness near the base of the denticles/teeth, i.e. showing no evidence for being 'socketed'. Given the possibility that the Rookery Limestone Member gnathal plates could be from either an acanthothoracid or *Lophosteus incrementus*, we assign them to Gnathostomata indet., although the acanthothoracid affinity seems most likely based on comparison with the plates of *Kosoraspis peckai*. No scales with the rhombic shape and keel-like swelling on the base that typify *Lophosteus* scales (Gross 1969, fig. 2) were identified in the Rookery Limestone Member sample residues, but the ornament on one plate fragment MMMC06290 (Fig. 5d, 5e) is comparable to that on some spine fragments from *L. superbus* (e.g., Gross 1969, figs. 3E1, 3I1, 5B2, 5C2). However, both *Lophosteus* and romundinids appear to have a vast range of dermal bone, and possibly also scale, ornamentation. One poorly preserved scale MMMC06291 (Fig. 5f) has inclined tubercular ornament similar to fragment MMMC06290. Scales MMMC06292and MMMC06293 (Fig. 5g–i) are most likely from placoderms, but nothing comparable is known from articulated fossils, or even as isolated elements.

CHONDRICHTHYES Huxley, 1880
ACANTHODII Owen, 1846 [sensu Burrow 2021]
Order, Family indet.

Genus *Nostovicina* Valiukevičius and Burrow, 2005

Type species
Nostovicina fragila (Valiukevičius, 2003).

Diagnosis
[scales] Body scales usually show superpositional growth; scale crowns may be flat and smooth to moderately

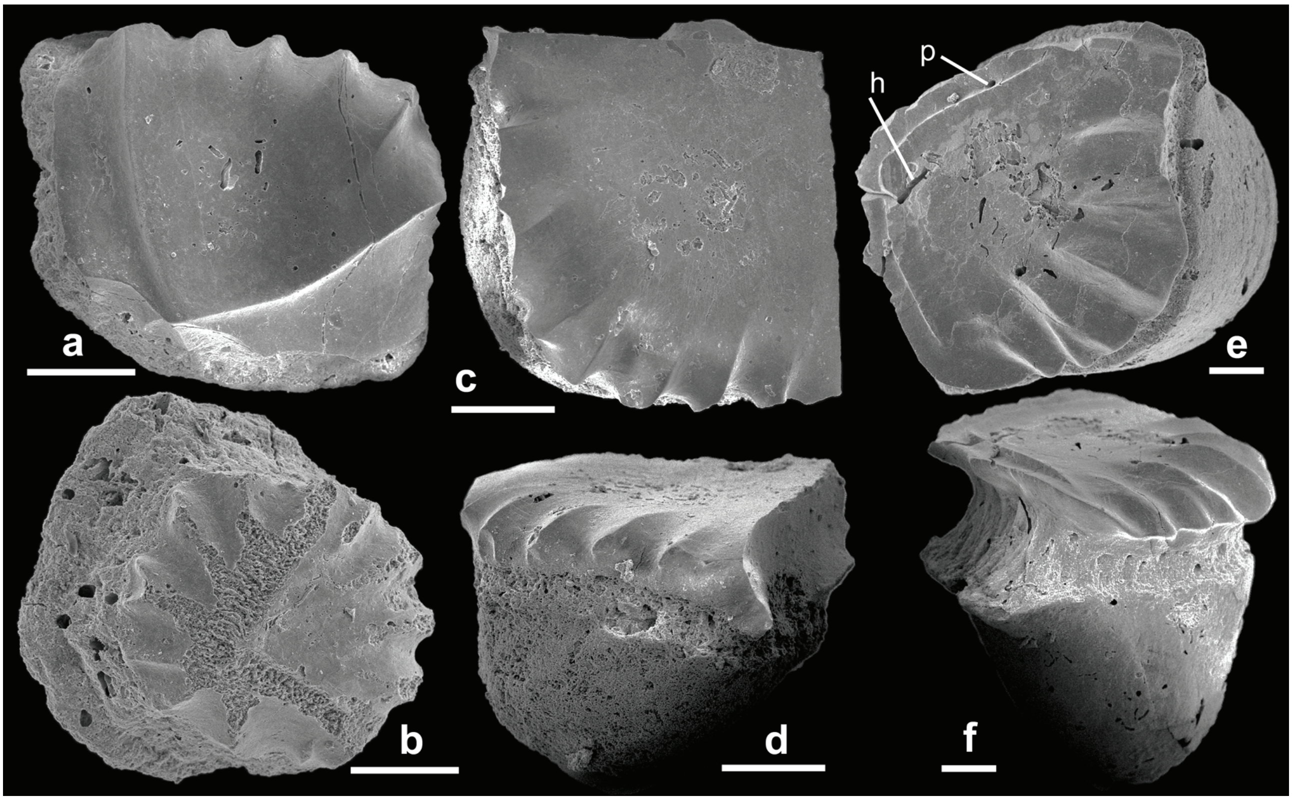

Figure 6. Acanthodian scales. a–d, *Nostovicina guangxiensis* (Wang, 1992); a, MMMC06294 (IY499-014); b, MMMC06295 (IY499-005). c, d, MMMC06296, c crown view (IY499-009), d, lateral view (IY499-025). e, f, *Trundlelepis cervicostulata* Burrow, 1997; MMMC06297, e, crown view (IY499-008), f, lateral view (IY499-024); h, hyphal boring; p, pore. All from sample C3474; scale bars = 100 µm.

inclined bearing subparallel, or rarely subradial, anterior ridges, which fade out posteriorly, and sometimes form a slightly raised medial area. Crowns of tesserae and scales are composed of a moderately cellular odontocytic mesodentine network mainly lacking enlarged vascular canals. Some species have thin layers of durodentine developed in outer laminae; Stranggewebe is lacking (after Burrow 2021).

Nostovicina guangxiensis **(Wang, 1992)**
Figure 6a, 6b, ?6c, ?6d

Diagnosis
Scale crowns have a central area with ridges of varying length radiating back from the anterior edge, and sharp oblique side ridges that converge towards the posterior corner of the crown. Rare, large scales have Stranggewebe developed low in the crown. The scale crown is smaller than the convex base. The embryonic zone is relatively small.

Referred material
Two scales MMMC06294 from sample C 3474 (IY499-014, Fig. 6a) and MMMC06295 from sample C 3474 (IY499-005, Fig. 6b), and possibly MMMC06296 from sample C 3474 (IY499-009, IY499-025, Fig. 6c, 6d).

Description
The better preserved scale MMMC06294 (Fig. 6a) is 0.45 mm wide and 0.33 mm long, the more eroded scale MMMC06295 (Fig. 6b) is c. 0.4 mm wide and 0.35 mm long. Both scales have a sub-triangular higher crown, with three or four short radial ridges running back from the anterior crown edge. Scale MMMC06295 has six or seven side crown ridges converging towards the posterior corner of the main crown, and scale MMMC06294 has four short subvertical ridges below the posterior corner of the crown, with smooth flat side ledges between the posterior corner and anterior crown edge. Both scales lack a constricted neck, and the crown is smaller than the base.

Scale MMMC06296 (Fig. 6c, 6d) is c. 0.4 mm long, 0.45 mm wide and 0.3 mm deep, with a smooth flat crown ornamented by eight short sharp ridges radiating back from the semicircular anterior edge of the crown. Sides of the crown are straight, converging at c. 95º at the posterior corner (Fig. 6c). The ridges curve down to the very short neck anteriorly, with the central ridges truncated (Fig. 6d). The dentinous tissue of the crown extends down close to the top of the base posteriorly (Fig. 6d). There is no rim between the crown-neck region and the base of the scale, which is tumid, and deeper than the crown+neck.

Remarks
This scale form was first recognized in Australia by Pickett *et al*. (1985), with scales from the Lochkovian 'Tumblong Oolite' assigned by those authors to *Nostolepis striata*. Scales of the same species from other Australian localities were subsequently assigned to various genera (see synonymy in Burrow 2002, p. 91), with the current combination *Nostovicina guangxiensis* nominated by Valiukevičius and Burrow (2005).

Comparison
Scales MMMC06294 and MMMC06295 are readily assignable to *N. guangxiensis*. Scale MMMC06296 lacks the distinctive side ridges that characterize most *N. guangxiensis* scales, but the relative dimensions of the base, neck and crown, and the crown ridge length and form are similar. The truncated anterior ends of the ridges on the central crown are also a feature seen on some *N. guangxiensis* scales (e.g., Burrow 2021, fig. 48E).

In eastern Australia, *Nostovicina guangxiensis* has a rather long stratigraphic range, being known from: the Lochkovian Connemarra Formation, Pragian 'Tumblong Oolite', and upper Pragian to lower Emsian Troffs Formation, New South Wales; the upper Lochkovian or lower Pragian Martins Well Limestone, north Queensland; the Pragian Coopers Creek Limestone and Emsian (*perbonus* CZ) Murrindal Limestone, Victoria; and the Pragian Point Hibbs Formation, Tasmania (Burrow 1997, 2002, 2021, Burrow *et al*. 1998). The type material is from the Emsian Ertang Formation, Guangxi, China (Wang 1992). The species is also recorded from the Pragian to lower Emsian Ganxi and Xiejiawan formations, Sichuan, China (Burrow *et al*. 2000) and the Lochkovian Enmakaj Formation, Chukotka, Russia (Mark-Kurik *et al*. 2013). As noted by Burrow (2021), scales of the purportedly late Silurian (Ludlow) *Yealepis douglasi* Burrow and Young, 1999 closely resemble those of *N. guangxiensis*. Recent investigations by Earp (2024) of the geology and fauna and flora from the type locality of *Yealepis*, near Yea, Victoria, cast doubts on the Ludlow age; a Lochkovian age might be more likely, in which case the two taxa could be synonymous.

Order ISCHNACANTHIFORMES Berg, 1940
Family PORACANTHODIDAE Vergoossen, 1997

Genus *Trundlelepis* Burrow, 1997

Type species
Trundlelepis cervicostulata Burrow, 1997

Trundlelepis cervicostulata **Burrow, 1997**
Figure 6e, 6f

Diagnosis
Small scales (0.15 - 0.8 mm wide), with a horizontal crown plane, four to twelve anterior radial ridges, eight to ten latero-posterior neck ribs or four to six canal pores above the posterior crown/neck junction, and a moderately large, convex base which can protrude forward of the anterior crown. Some scales have up to six pore canals opening on the posterior crown surface (after Burrow 2002, scale morphology).

Referred material
Scale MMMC06297 from sample C 3474 (IY499-08, IY499-08, Fig. 6e, 6f).

Description
The solitary scale MMMC06297 assigned to this taxon is 0.6 mm long, 0.8 mm wide, and 0.6 mm high, with the base markedly deeper than the crown plus neck.

The crown bears six sharp ridges radiating out for less than half the length of the crown from its anterior edge, with one ridge bifurcating near towards this edge. The presumed outermost crown growth zone is clearly marked posteriorly, stepped down from the inner growth zone. One or two pores open out onto the crown surface near this boundary (Fig. 6e). The posterior neck bears ten vertical ribs (Fig. 6f).

Comparison

The scale is comparable with the *T. cervicostulata* holotype scale MMMC02239 (Burrow 1997, pl. 3 fig. 11; 2002, fig. 32A, B), mainly differing in having crown pore openings like those visible in paratype scale MMMC02234 (Burrow 1997, pl. 3 fig. 3; Burrow 2002, fig. 32C). In Australia, *T. cervicostulata* has a stratigraphic range from the upper Lochkovian through the Pragian, being found in the Connemarra and Gleninga formations and 'Tumblong Oolite' in New South Wales, upper Lochkovian or lower Pragian Martins Well Limestone in Queensland, lower Pragian Point Hibbs Formation in Tasmania, and possibly the Pragian Waratah and Pragian Coopers Creek limestones in Victoria (see Burrow 2021 for details).

DISCUSSION

The 'placoderm' taxa identified in the suite of microvertebrate remains from the Rookery Limestone Member support the Lochkovian age inferred from the co-occurring conodont taxa. Romundinid placoderms are almost exclusively known from Lochkovian deposits worldwide, in the Arctic Canadian Archipelago and Northwest Territories, Canada; Nevada, USA; Pechora, Norilsk, and Novaya Sibir Island, Russia; central New South Wales, Australia; and possibly Celtiberia, Spain and western Tasmania, Australia, the latter being the only post-Lochkovian record. In central New South Wales, the placoderm *Connemarraspis* is only known from Lochkovian limestones, but has also been found in the early Pragian (*sulcatus* CZ) of western Tasmania; no other occurrences are known. The acanthodian taxa *Nostovicina guangxiensis* and *Trundlelepis cervicostulata* have a longer stratigraphic range, with *N. guangxiensis* found from the Lochkovian to the lower Emsian, and *T. cervicostulata* from the Lochkovian to Pragian.

ACKNOWLEDGMENTS

Carole Burrow acknowledges the provision of basic facilities by the Queensland Museum. The field work in the area in May 2024 was supported by the Geological Survey of NSW (Zhen) and the Australian Museum (Smith). Patrick Dwyer (GSNSW) and Harry Langford (Honours student, University of Wollongong) are thanked for their help during the field work. Samples were processed (acid leaching and residue separation) at the Palaeontology Lab of GSNSW, Londonderry with assistance of Mark Ryland. SEM study of vertebrate remains and conodonts was undertaken at the Electron Microscope Unit of the Macquarie University with assistance from Sue Lindsay. Cassie Yarnold (GSNSW) is thanked for final drafting of Figure 1. Anonymous reviewers are acknowledged for their careful and constructive comments on the manuscript. Yong Yi Zhen publishes with the permission of the Chief Geoscientist & Head of the Geological Survey of New South Wales.

REFERENCES

Andrews, E.C. (1913 for 1911). Report on the Cobar Copper and Gold-Field. Part 1. *Geological Survey, New South Wales Department of Mines, Mineral Resources* **17**, 1–207.

Basden, A., Burrow, C.J., Hocking, M., Parkes, R. and Young, G.C. (2000). Siluro-Devonian microvertebrates from south-eastern Australia, *Courier Forschungsinstitut Senckenberg* **223**, 201–222.

Berg, L.S. (1940). Classification of fishes both recent and fossil. *Trudy Zoologischeskogo Instituta* **5**, 85–517 (in Russian).

Bischoff, G. and Sannemann, D. (1958). Unterdevonische Conodonten aus dem Frankenwald. *Notizblatt des Hessischen Landesamtes Bodenforsch* **86***,* 87–110.

Branson, E.B. and Mehl, M.G. (1933). Conodont studies No. 1: Conodonts from the Harding Sandstone of Colorado; Bainbridge (Silurian) of Missouri; Jefferson City (Lower Ordovician) of Missouri. *University of Missouri Studies* **8** (1), 7–72.

Brazeau, M.D., Giles, S., Dearden, R.P., Jerve, A., Ariunchimeg, Y., Zorig, E., Sansom, R., Guillerme, T. and Castiello, M. (2020). Endochondral bone in an Early Devonian 'placoderm' from Mongolia. *Nature Ecology & Evolution* **4**, 1477–1484.

Brazeau, M.D., Yuan, H., Giles, S., Jerve, A.L., Zorig, E., Ariunchimeg, Y., Sansom, R.S. and Atwood, R.C. (2023). A well-preserved 'placoderm' (stem-group Gnathostomata) upper jaw from the Early Devonian of Mongolia clarifies jaw evolution. *Royal Society Open Science* **10**, 221452.

Burrow, C.J. (1995). A new lophosteiform (Osteichthyes) from the Lower Devonian of Australia. *Geobios Mémoire Spécial* **19**, 327–333.

Burrow, C.J. (1996). Placoderm scales from the Lower Devonian of New South Wales, Australia. *Modern Geology* **20**, 351–369.

Burrow, C. J. (1997). Microvertebrate assemblages from the Lower Devonian (*pesavis*/*sulcatus* zones) of central New South Wales, Australia. *Modern Geology* **21**, 43–77.

Burrow, C.J. (2002). Lower Devonian acanthodian faunas and biostratigraphy of south-eastern Australia. *Memoirs of the Association of Australasian Palaeontologists* **27**, 75–137.

Burrow, C.J. (2003a). Earliest Devonian gnathostome microremains from central New South Wales (Australia). *Geodiversitas* **25**, 273–288.

Burrow, C.J. (2003b). Comment on "Separate Evolutionary Origins of Teeth from Evidence in Fossil Jawed Vertebrates". *Science* **300**, 1661b.

Burrow, C.J. (2006). Placoderm fauna from the Connemarra Formation (?late Lochkovian, Early Devonian), central New South Wales. *Alcheringa* **30**, 59–88.

Burrow, C. (2021). *Handbook of Paleoichthyology*. *Vol. 5. Acanthodii, Stem Chondrichthyes*. (Verlag Dr Friedrich Pfeil: Munich).

Burrow, C.J. and Turner, S. (1999). A review of placoderm scales, and their relevance in placoderm phylogeny. *Journal of Vertebrate Paleontology* **19**, 204–219.

Burrow, C.J. and Young, G.C. (1999). An articulated teleostome fish from the Late Silurian (Ludlow) of Victoria, Australia.

Records of the Western Australian Museum Supplement **57**, 1–14.

Burrow, C., Hu, Y. and Young, G. (2016). Placoderms and the evolutionary origin of teeth: a comment on Rucklin & Donoghue (2015). *Biology Letters* **12**, 27677820.

Burrow, C.J., Long, J.A. and Turner, S. (1998). Lower Devonian microvertebrates from Tasmania. *Alcheringa* **22**, 9–20.

Burrow, C.J., Turner, S. and Wang, S.-T. (2000). Devonian microvertebrates from Longmenshan, Sichuan, China: Taxonomic assessment. *Courier Forschungsinstitut Senckenberg* **223**, 391–452.

Burrow, C.J., Turner, S. and Young, G.C. (2010). Middle Palaeozoic microvertebrate assemblages and biogeography of East Gondwana (Australasia, Antarctica). *Palaeoworld* **19** (1), 37–54.

Coates, M.I., Finarelli, J.A., Sansom, I.J., Andreev, P.S., Criswell, K.E., Tietjen, K., Rivers, M.L. and La Riviere, P.J. (2018). An early chondrichthyan and the evolutionary assembly of a shark body plan. *Proceedings of the Royal Society B: Biological Sciences* **285**, 20172418.

Colquhoun, G.P., Hughes, K.S., Deyssing, L., Ballard, J.C., Phillips, G., Troedson, A.L., Folkes, C.B. and Fitzherbert, J.A. (2024). New South Wales Seamless Geology Dataset, Version 2.4 [Digital Dataset]. Geological Survey of New South Wales, Maitland, NSW.

David, V. (2005). *Structural Setting of Mineral Deposits in the Cobar Basin*. University of New England, Armidale (unpublished PhD thesis).

Denison, R.H. (1978). *Placodermi*. In 'Handbook of Paleoichthology, Volume 2' (Ed. H.-P. Schultze). 128 pp. (Gustav Fischer Verlag: Stuttgart and New York).

Downes, P.M., Blevin, P.L., Armstrong, R., Simpson, C.J., Sherwin, L., Tilley, D.B. and Burton, G.R. (2016). Outcomes of the Nymagee mineral system study – an improved understanding of the timing of events and prospectivity of the central Lachlan Orogen. *Quarterly Notes of the Geological Survey of New South Wales* **147**, 1–38.

Druce, E.C. (1970). Conodonts from the Garra Formation (Lower Devonian) New South Wales, Australia. *Bureau of Mineral Resources Geology and Geophysics Bulletin* **116**, 29–63.

Earp, C. (2024). Notanopliid brachiopods and associated fossils from the Yea area, central Victoria: a key to resolving age and correlation problems in a complex geological setting. *Proceedings of the Royal Society of Victoria* **136**, RS23021.

Felton, E.A. (1981). *Geology of the Canbelego 1:100 000 sheet, 8134*. Geological Survey of New South Wales, Sydney, 119 p.

Gegenbaur, C. (1874). *Manuel d'anatomie comparée*. (Simon Raçon et Comp.: Paris).

Glen, R.A. (1994). *Geology of the Cobar 1:100 000 Sheet 8035*, 2nd edition, Geological Survey of New South Wales, Sydney.

Glen, R. A. (1995). Thrusts and thrust-associated mineralisation in the Lachlan Orogen. *Economic Geology* **90**, 1402–1429.

Goujet, D. and Young, G.C. (2004). *Placoderm anatomy and phylogeny: new insights*. In 'Recent Advances in the Origin and Early Radiation of Vertebrates' (Eds G. Arratia, M.V.H. Wilson and R. Cloutier). pp. 109–126. (Verlag Dr Friedrich Pfeil: Munich).

Gross, W. (1959). Arthrodiren aus dem Obersilur der Prager Mulde. *Palaeontographica A* 113, 1–35.

Gross, W. (1969). *Lophosteus superbus* Pander, ein Teleostome aus dem Silur Oesels. *Lethaia* **2**, 15–47.

Hu, Y.-Z., Young, G.C., Burrow, C., Zhu, Y.-a. and Lu, J. (2019). High resolution XCT scanning reveals complex morphology of gnathal elements in an Early Devonian arthrodire. *Palaeoworld* **28**, 525–534.

Huxley, T.H. (1880). On the application of the laws of evolution to the arrangement of the Vertebrata and more particularly the Mammalia. *Proceedings of the Zoological Society of London* **43**, 649–662.

Johanson, Z. and Smith, M.M. (2003). Placoderm fishes, pharyngeal denticles, and the vertebrate dentition. *Journal of Morphology* **257**, 289–307.

Jones, S.L., Fitzherbert, J.A., Waltenberg, K. and Bodorkos, S. (2020). New SHRIMP U-Pb ages from the Cobar Basin, New South Wales: Mineral Systems projects, July 2018-June 2019. *Geoscience Australia, Record* **2020/42**, 1–75.

Klapper, G. and Philip, G.M. (1971). Devonian conodont apparatuses and their vicarious skeletal elements. *Lethaia* **4**, 429–452.

Mark-Kurik, E. (1994). Placoderms and their stratigraphical significance. In *Stratigraphy and Fauna of the Lower Devonian of the Tareya Key Section (Taimyr)* (In Russian) (Eds S. Cherkesova, V. Karatajute-Talimaa and R. Matukhin). pp. 123–132. (Nedra: St Petersburg).

Mark-Kurik, E., Blieck, A., Burrow, C.J. and Turner, S. (2013). Early Devonian fishes from coastal De Long Strait, central Chukotka, Arctic Russia. *Geodiversitas* **35**, 545–578.

Mathieson, D., Mawson, R., Simpson, A. and Talent, J. (2016). Late Silurian (Ludlow) and Early Devonian (Pragian) conodonts from the Cobar Supergroup, western New South Wales, Australia. *Bulletin of Geosciences* **91**, 583–652.

M'Coy, F. (1848). I.—On some new fossil fish of the Carboniferous Period. *Annals and Magazine of natural History* **2**, 1–10.

Murphy, M.A. and Matti, J.C. (1982). Lower Devonian conodonts *(hesperius-killdlei* zones), Central Nevada. *University of California Publications in the Geological Sciences* **123**, 1–83.

Olive, S., Kotoulas, I., Goujet, D., Donoghue, P.C.J., Marone, F. and Rücklin, M. (2025). A new 'acanthothoracid' placoderm from the Arctic Canada (Early Devonian) and its bearing on the evolution of jaws and teeth. *Royal Society Open Science* **12**, 250837.

Ørvig, T. (1975). Description, with special reference to the dermal skeleton, of a new radotinid arthrodire from the Gedinnian of arctic Canada. *Colloques Internationaux du Centre National de la Recherche Scientifique* **218**, 41–71.

Owen, R. (1846). *Lectures on the comparative anatomy and physiology of the vertebrate animals delivered at the Royal College of Surgeons, England in 1844 and 1846. Part I, Fishes*. (Longman, Brown, Green and Longmans: London).

Parkes, R. (1995). Late Silurian-Early Devonian vertebrate microremains from Nevada and southeastern Australia: biochronology, biogeography and application of novel histological techniques. Honours thesis, Macquarie University.

Philip, G.M. (1965). Lower Devonian conodonts from the Tyers area, Gippsland, Victoria. *Proceedings of the Royal Society of Victoria* **79**, 95–117.

Pickett, J.W. (1980). Conodont assemblages from the Cobar Supergroup (Early Devonian), New South Wales. *Alcheringa* **4**, 67–88.

Pickett, J.W., Turner, S. and Myers, B. (1985). The age of marine sediments near Tumblong, southwest of Gundagai. *Geological Survey of NSW Quarterly Notes* **58**, 12–15.

Pogson, D.J. and Felton, E.A. (1978). Reappraisal of geology, Cobar-Canbelego-Mineral Hill region, central western New South Wales. *Quarterly Notes of the Geological Survey of New South Wales* **33**, 1–14.
Rücklin, M. and Donoghue, P.C.J. (2015). *Romundina* and the evolutionary origin of teeth. *Biology Letters* **11**, 20150326.
Smith, M.M., Clark, B., Goujet, D. and Johanson, Z. (2017). Evolutionary origins of teeth in jawed vertebrates: conflicting data from acanthothoracid dental plates ('Placodermi'). *Palaeontology* **60**, 829–836.
Stensiö, E. (1944). Contributions to the knowledge of the vertebrate fauna of the Silurian and Devonian of western Podolia. II. Notes on two arthrodires from the Downtonian of Podolia. *Arkiv för Zoologi* **35**, 1–83.
Turner, S. and Murphy, M.A. (1988). Early Devonian vertebrate microfossils from the Simpson Park Range, Eureka County, Nevada. *Journal of Paleontology* **62**, 959–964.
Valenzuela-Ríos, J.I., Liao, J.C. and Calvo, H. (2017). Middle and upper Lochkovian (Lower Devonian) at Segre 4 section. *Berichte des Institutes für Erdwissenschaften der Karl-Franzens-Universität Graz* **23**, 61–64.
Valiukevičius, J.J. (2003). Devonian acanthodians from Severnaya Zemlya Archipelago (Russia). *Geodiversitas* **25**, 131–204.
Valiukevičius, J. and Burrow, C.J. (2005). Diversity of tissues in acanthodians with "*Nostolepis*"-type histological structure. *Acta Palaeontologica Polonica* **50**, 635–649.
Vaškaninová, V., Chen, D., Tafforeau, P., Johanson, Z., Ekrt, B., Blom, H. and Ahlberg, P.E. (2020). Marginal dentition and multiple dermal jawbones as the ancestral condition of jawed vertebrates. *Science* **369**, 211–216.
Wang, R. (1993). Taxonomie, Palökologie und Biostratigraphie der Mikroichthyolithen aus dem Unterdevon Keltiberiens, Spanien. *Courier Forschungsinstitut Senckenberg* **161**, 1–205.
Wang, N.-Z. (1992). Microremains of agnathans and fishes from Lower Devonian of Central Guangxi with correlation of Lower Devonian between Central Guangxi and Eastern Yunnan, South China. *Acta Palaeontologica Sinica* **31**, 298–307.
Wells, J.W. (1944). Fish remains from the Middle Devonian Bone Beds of the Cincinnati Arch region. *Palaeontographica Americana* **3**, 99–160.
Zhen, Y.Y., Smith, P.M., Zhang, Y.D., Strusz, D.L., Percival, I.G., Burrow, C.J., Rutledge, J. and Trigg, S.J. (2023). Field guide and catalogue of Ordovician–Devonian fossils from the Cargelligo and Nymagee 1:250 000 geological mapping area, central New South Wales. *Quarterly Notes of the Geological Survey of New South Wales* **157**, 1–84.
Ziegler, W. (1960). Conodonten aus dem rheinischen Unterdevon (Gedinnium) des Remscheider Sattels (Rheinisches Schiefergebirge). *Palaeontologische Zeitschrift* **34***,* 169–201.